# Degradation mechanism due to decomposition of organic electrolyte in Li/MoS$_2$ cells during long cycling

Kazuma Kumai [a], Tomohiko Ikeya [a], Kaoru Ishihara [a], Toru Iwahori [a], Nobuyuki Imanishi [b], Yasuo Takeda [b], Osamu Yamamoto [b,*]

[a] Central Research Institute of Electric Power Industry (CRIEPI), 2-11-1 Iwado Kita, Komae-shi, Tokyo 201, Japan
[b] Department of Chemistry, Faculty of Engineering, Mie University, Kamihama-cho, Tsu 514, Japan

## Abstract

The degradation mechanism due to the decomposition of organic electrolytes during charge and discharge cycling of Li/MoS$_2$ cells has been investigated. The gas products of the electrolyte decomposition during long cycling were measured by gas chromatography (GC), and the changes of electrolyte composition was measured by gas chromatography/mass spectrometry (GC/MS). The gases were produced through two types of electrolyte decomposition: the electrochemical reaction, which was dependent on the charge and discharge voltage, and the chemical reaction, which was independent of the discharge voltage. This decomposition of electrolytes occurred under a discharge voltage lower than 1.4 V. The operating conditions with a lower discharge rate and a deeper depth of discharge (D.O.D.) accelerated the electrochemical decomposition. The rate of gas production by chemical decomposition, which is independent of the discharge condition, was estimated to be about 0.1 ml/h. © 1998 Elsevier Science S.A.

Keywords: Secondary lithium cells; Degradation mechanism; Electrolyte decomposition; Cycle life

## 1. Introduction

Lithium (Li) secondary batteries are very attractive as electric power storage devices because of their high energy density and long cycle life. They have been used as power supplies for portable electric devices, and are expected to be used as energy storage systems for load leveling and as power sources for electric vehicles. For practical use of batteries for electric energy storage, it is necessary to prolong the cycle life (more than 3500 cycles) and improve the safety. One of the problems in Li secondary batteries is the decomposition of organic electrolytes during cycling. The nonaqueous organic electrolytes decompose to produce gaseous products by charge and discharge cycling. The reaction between organic electrolyte solutions and Li not only consumes the active Li in the cell but also increases the internal pressure. High internal pressure can lead to safety hazards during practical use. In the carbon anode Li batteries, it was reported that degradation of the

organic electrolyte with gas generation occurred during the first charging [1] and overcharging [2]. Also, an electrochemical reduction of propylene carbonate (PC) at the cathode in a rechargeable LiAsF$_6$–PC Li/MoS$_2$ system has been reported [3].

A Li secondary cell using MoS$_2$ as the cathode has been examined extensively for many years [4,5] because it has been commercialized as the first practical Li rechargeable battery [6]. Laman and Brandt [7] reported that the cycle life of the Li/MoS$_2$ cell was limited by electrolyte degradation. However, the degradation mechanism is still not well understood.

In this work, in order to investigate the degradation mechanism of the Li/MoS$_2$ cell, we carried out cycle life tests and simultaneously analyzed the composition of generated gases.

## 2. Experimental

An AA-size Li/MoS$_2$ cell with 0.6 A · h nominal capacity purchased from Moli Energy was used for cycle life tests. It has a metallic Li anode and a beta Li molybde-

* Corresponding author. Department of Chemistry, Mie University, 1515 Kamihama-cho, Tsu, Mie 514, Japan.
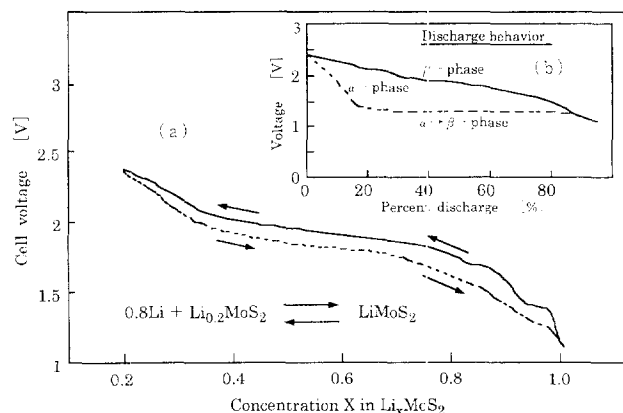
Fig. 1. Voltage $V$ vs. $X$ of Li/Li$_x$MoS$_2$ cell charging (————) and discharging (—) at a 15.0 h rate. The data are normalized to $X = 0.2$ at 2.4 V and $X = 1.0$ at 1.1 V.

num sulfide ($\beta$-Li$_x$MoS$_2$) cathode [6,8]. The electrolyte consisted of a 1.0 M solution of LiAsF$_6$ in a mixture of 50:50 percent by volume of ethylene carbonate (EC) and PC.

Fig. 1a shows the voltage for the Li/$\beta$-Li$_x$MoS$_2$ electrochemical cell as a function of the Li concentration at 25°C. The cell was discharged and recharged at a 15.0 h rate (40 mA) between 2.4 and 1.1 V. The values of $x$ have been normalized to $x = 0.2$ at 2.4 V and $x = 1.0$ at 1.1 V. The cells show sloping charge and discharge curves and an open circuit voltage that decreases from 2.4 V for a fully charged cell to 1.1 V for a fully discharged cell with an average voltage of 1.8 V.

The typical cell reaction is as follows.

$$0.8Li + \beta - Li_{0.2}MoS_2 \rightleftarrows \beta - LiMoS_2 \, (0.2 < x \leq 1)$$
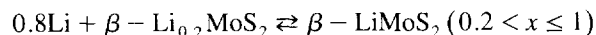
The molybdenum sulfide of the cathode normally exists in a crystalline phase known as $\beta$-MoS$_2$ (high capacity structure). If, however, a cell is operated at above 2.0 V, some of the $\beta$-MoS$_2$ changes to a different phase, $\alpha$-MoS$_2$ (low capacity structure: $0 < x \leq 0.2$). As is shown in Fig.

1b, $\alpha$-MoS$_2$ has a different, lower discharge curve until the cell potential reaches 1.3 V, at which point the alpha phase changes back to the beta phase, and remains at constant voltage until the transition is complete.

The cells were charged at the constant rate of 0.1 C (0.24 mA/cm$^2$). It is well known that higher rates of charging current accelerate the formation of Li dendrites [9,10]. The charge cut-off voltage was selected as 2.4, 2.2 and 2.0 V. The cells were discharged up to depth of discharge (D.O.D.) at discharge rates of 0.1 and 0.3 C.

The test conditions and summary of the cycle test results are given in Table 1.

After the test run, the cells were set up in a glove bag (constant volume of 40 l) filled with high-purity dry argon gas, and the generated gases in the cell were released into a bag using a Minitor cutter (Minimo, model C730).

The gases were analyzed by GC with a flame ionization detector (FID). Separators were removed from the cells and immersed in organic solvent (dichloromethane, 2 ml) for 1 h. The chemical composition of the electrolyte solution was determined by gas chromatography/mass spectrometry (GC/MS).

## 3. Results and discussion

### 3.1. Dependence of the coulombic efficiency on the discharge cut-off voltage

Fig. 2 shows the relationship between the apparent coulombic efficiencies and discharge cut-off voltages in initial capacity tests as a function of the charge cut-off voltage. The cells were charged at 0.1 C to 2.0, 2.2 and 2.4 V, and discharged at 0.125 C to the terminated discharge voltage. The coulombic efficiency was defined as the ratio of the amount of discharge and charge in coulombs of the cells. The coulombic efficiency was dependent on the terminated discharge voltage for each charge cut-off volt-

Table 1
The summary of test conditions and results under different D.O.D. with charge cut-off voltages of 2.0, 2.2 and 2.4 V

| D.O.D. (%) | Charge cut-off voltage (V) | Discharge conditions | | Cycle number | Cycle life | Integrated capacity (A·h) | Generated gas volume (ml) | Accumulated discharge time below 1.4 V (h) |
| --- | --- | --- | --- | --- | --- | --- | --- | --- |
| | | Rate (C) | Time (h) | | | | | |
| 100 | 2.4 | 0.1 | 10.0 | 93 | 83 | 48 | 27.5 | 43.8 |
| | | 0.3 | 3.3 | 358 | 252 | 119 | 5.7 | 77.5 |
| 80 | 2.2 | 0.1 | 8.0 | 175 | 153 | 73 | 21.8 | 43.6 |
| | | 0.3 | 2.7 | 564 | 526 | 237 | 4.8 | 58.6 |
| 50 | 2.0 | 0.1 | 5.0 | 272 | 215 | 64 | 13.4 | 118.7 |
| | | 0.3 | 1.7 | 1148 | 1110 | 431 | 18.7 | 162.0 |
| 30 | 2.0 | 0.1 | 3.0 | 411 | 380 | 67 | 4.8 | 58.4 |
| | | 0.3 | 1.0 | 2716 | 2620 | 468 | 17.5 | 145.7 |

The cells were charged at the constant rate of 0.1 C. Rest time: 1 h after charge and discharge. D.O.D. 100% corresponds to 0.6 A·h discharge. The cycle life was defined as the cycle when discharge capacity decreased to 80% of its initial capacity or when the energy efficiency fell to 80%.
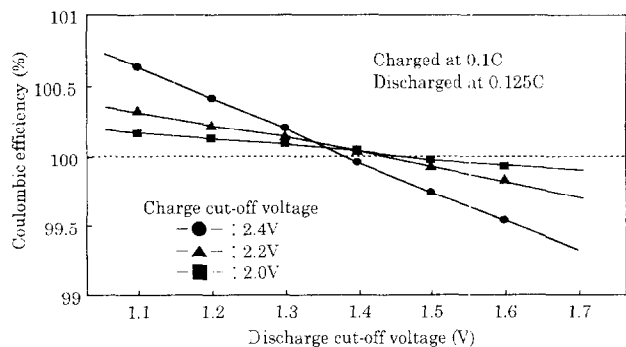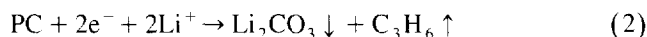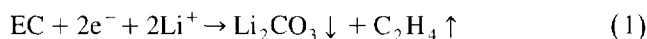
Fig. 2. The dependence of the coulombic efficiency on the terminated discharge cut-off voltage.

age of 2.0, 2.2 and 2.4 V. The efficiency increased with decreasing terminated discharge voltage. At each charge cut-off voltage, 100% coulombic efficiency is observed at around a 1.35 V terminated discharge voltage. The excess coulombs passed during discharge may correspond to the electrolyte decomposition on the cathode in the lower discharge voltage region. Higher charge voltages shows a change in the ratio due to the phase transformation from $\beta$-MoS$_2$ to $\alpha$-MoS$_2$ and the excess coulombic efficiency at lower discharge voltages could be related to the magnitude of electrolyte decomposition. The phase transition was accompanied by electrolyte decomposition on the cathode [3]. This decomposition would contribute to the apparent coulombic efficiency of over 100%.

In the region of discharge below 1.4 V, the electrolyte decomposition at the cathode occurs as follows.

$$EC + 2e^- + 2Li^+ \rightarrow Li_2CO_3 \downarrow + C_2H_4 \uparrow \qquad (1)$$

$$PC + 2e^- + 2Li^+ \rightarrow Li_2CO_3 \downarrow + C_3H_6 \uparrow \qquad (2)$$

These reactions occur at the electrode–electrolyte interface [3], and the reaction of PC and EC with Li produce Li carbonate (Li$_2$CO$_3$), propylene (C$_3$H$_6$) and ethylene (C$_2$H$_4$). These reactions reduce ionic conductivity of the electrolyte through solvent depletion, accumulation of products on the electrode and increase of internal pressure due to the generated gas. Therefore, degradation of the electrolyte solution causes the decrease in the cell discharge capacity.
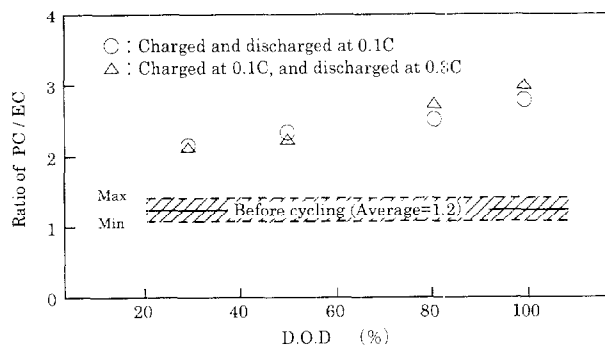
## 3.2. Gas generation with decomposition of electrolyte during cycling

The composition of electrolytes in the cells after cycle testing was determined by GC/MS. No components, other than PC and EC were detected. However, the ratio of electrolyte components (PC, EC) was dependent on the cycle test conditions. The relationship between the PC:EC ratio and D.O.D. is shown in Fig. 3. Before cycling, the PC:EC ratio ranged from 1.0 to 1.3, and increased to the range of 2 to 3 after the cycle tests. The ratio increased with increasing D.O.D.. This change of the PC:EC ratio suggests a difference in the reaction rates between Eqs. (1) and (2).

Gaseous products generated by electrolyte decomposition were measured by GC. The generated gas mainly consisted of propylene and ethylene. Trace quantities of methane, ethane and propane were also detected. The total volume of gas in the cycled cells was in the range of 4–30 ml. The relationship between the ratio of ethylene and propylene gases generated by electrolyte decomposition and D.O.D. after the cycle tests is shown in Fig. 4. The ratio is approximately 1 for the shallow D.O.D. (30–50%), and increases to 2 to 3 for deep D.O.D. (80–100%). The relation was not dependent on the discharge current.

These results suggest that EC and PC decomposed electrochemically through Eqs. (1) and (2) for deep D.O.D.

## 3.3. Degradation mechanism due to decomposition of electrolyte solution

To determine the correlation between charge/discharge voltage and gas generation, cells were charged at 0.1 C and discharged at 0.125 C under the different cut-off voltages and number of cycles shown in Table 2. In the case of the terminated discharge voltage of 1.6 V, generation of gas was found to be almost prevented. However, in the case of the terminated discharge voltage of 1.1 V, a large amount of gas was generated. This result suggests that the electrolyte decomposition rate increased as the cell was discharged to a lower voltage.



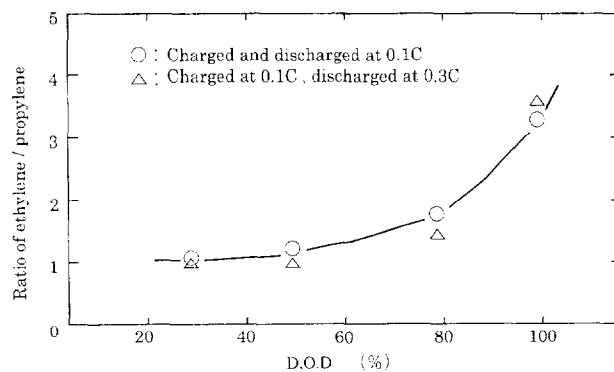Fig. 3. The PC:EC ratio vs. D.O.D. curves after cycle tests.



Fig. 4. The dependence of the ratio of ethylene and propylene in the decomposition gas of electrolytes on D.O.D..

Table 2
The cut-off charge/discharge voltage and amount of generated gases for various depths of discharge

| Voltage range (V) | D.O.D. (%) | Cycle number | Generated volume (ml) |
|---|---|---|---|
| 2.2–1.1 | 80 | 171 | 19.1 |
| 2.2–1.6 | 70 | 198 | 1.4 |
| 2.0–1.6 | 50 | 263 | 3.2 |

Cells were discharged at 0.125 C and charged at 0.1 C.

In order to estimate the magnitude of electrolyte decomposition, the rate per hour was calculated as the generated gas volume in the cell divided by the accumulated discharge time below 1.4 V for each cell. The relation between the rate of electrolyte decomposition and D.O.D. fell into three categories as shown in Fig. 5. They are (a) charging and discharging at 0.1 C to shallow D.O.D. (30–50%), (b) charging at 0.1 C and discharging at 0.3 C to deeper D.O.D. (80–100%), and (c) the charging and discharging at 0.1 C to deeper D.O.D. (80–100%).

The decomposition that occurs at the electrodes can either be a voltage dependent reaction (electrochemical) or a voltage independent reaction (chemical) [8]. Because of the voltage dependence, the electrochemical reaction takes place only at the cathode–electrolyte interface.

In the cases of (a) and (b), chemical reaction, the rate of gas generation is independent of D.O.D. and discharge rate, and was estimated to be about 0.1 ml/h.

In the case of (c), electrochemical reaction, the rate of gas generation strongly depend on D.O.D. and a high rate of gas generation is observed. This could not be explained in terms of discharge time below 1.4 V.

Fig. 6 shows the relation of terminated discharge voltages at discharge rates of 0.1 C and 0.3 C with the number of cycles. Cells were charged at 2.4 V and discharged with a constant capacity of 0.3 A · h. The terminated discharge voltage at a discharge rate of 0.3 C after the 20th cycle gradually decreased to 1.1 V. The terminated voltage at 0.1 C remained constant at around 1.4 V until nearly the end of the test. The behavior of the terminated discharge
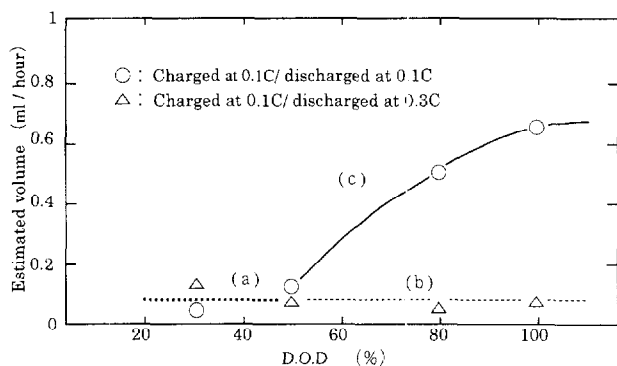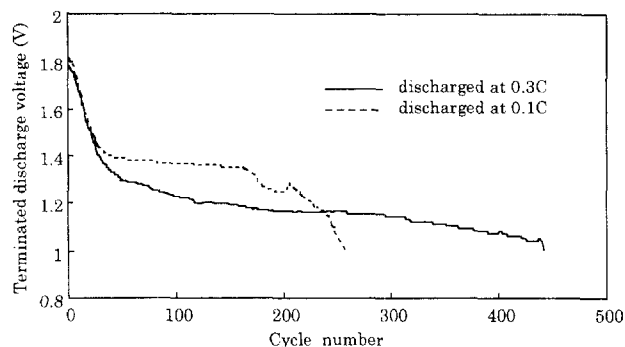


Fig. 6. Change in terminated discharge voltage as a function of cycle number.

voltage at 0.1 C after about the 20th cycle suggests that the transformation from $\alpha$-MoS$_2$ to $\beta$-MoS$_2$ occurred in the cathode. Transformation to $\beta$-MoS$_2$ accelerates the production of gas in the reaction of the electrolyte with the cathode. The phase transformation to the $\beta$-phase acts as a catalyst for electrolyte decomposition at the cathode.

From the results shown in Figs. 5 and 6, the electrolyte decomposition process of Li/MoS$_2$ cells is considered as follows. A partial phase transformation from $\beta$-MoS$_2$ to $\alpha$-MoS$_2$, which occurs at a charge voltage above 2.0 V, gradually reduces the cathode capacity. At the low capacity structure, $\alpha$-MoS$_2$ changes back to the $\beta$-MoS$_2$ below 1.4 V cathode potentials during low discharge rate. The electrolyte decomposition occurs in the cathode/electrolyte interface, and the phase transformation to $\beta$-MoS$_2$ accelerates the electrolyte decomposition reaction at low discharge currents. The total amount of electrolyte decomposition during discharge increases at low discharge current because of the longer discharge time. At a low discharge rate and deeper D.O.D., the decomposition of the electrolyte is the predominant process. It can be pointed out that a significant portion of the electrolyte decomposition occurs during discharge.

Without the phase transformation to $\beta$-MoS$_2$ during discharge, the amount of electrolyte decomposition is constant for the entire discharge time at low cathode potentials, and independent of the D.O.D. and the discharge current.

## 4. Conclusions

The role of organic electrolyte decomposition during the charge and discharge cycling in the degradation mechanism of a Li secondary battery was examined. In this experiment, gas was produced by the parasitic decomposition of electrolytes on the MoS$_2$ cathode. The decomposition mechanism consisted of two kinds of reactions. One is an electrochemical reaction which depends on charged and discharged voltages and is considered to be accelerated by



Fig. 5. The effect of D.O.D. on estimated volume of gases generated by electrolyte decomposition at discharge currents of 0.1 C and 0.3 C.

the phase transformation of the active cathode material. In this case, the decomposition rate for EC is found to be about three times greater than that for PC. The other one is a chemical reaction, which was independent of the discharge voltage. The rate of gas production per discharge time below 1.4 V is estimated to be about 0.1 ml/h, independent of discharge conditions.

## Acknowledgements

## References

[1] Z.X. Shu, R.S. McMillan, J.J. Murray, J. Electrochem. Soc. 140 (1993) 922.
[2] E. Cattaneo, J. Ruch, J. Power Sources 43–44 (1993) 341.
[3] R. Fong, M.C. Reid, R.S. McMillan, J.R. Dahn, J. Electrochem. Soc. 134 (1987) 516.
[4] C. Julien, T. Sekine, M. Balkanski, Solid State Ionics 48 (1991) 225.
[5] N. Imanishi, Y. Imanaka, Y. Takeda, O. Yamamoto, The 29th Battery Symp. in Japan, Extended Abstracts, 3B01 (1988) p. 257.
[6] R.R. Haering, J.A.R. Stiles, K. Brandt. US Patent (1982), No. 4,281,048.
[7] F.C. Laman, K. Brandt, J. Power Sources 24 (1988) 195.
[8] M.A. Py, R.R. Haering, Can. J. Phys. 61 (1983) 76.
[9] V.R. Koch, J.H. Young, Science 204 (1979) 499.
[10] K. Kumai, K. Ishihara, T. Iwahori, T. Tanaka, Proc. Electrochem. Soc. 93 (3) (1991) 371.